Using Atomic Force Microscopy to Study Nucleosome Remodeling on Individual Nucleosomal Arrays in Situ

H. Wang,* R. Bash,*[†] J. G. Yodh,[‡] G. Hager,[§] S. M. Lindsay,*[†][¶] and D. Lohr[†]

*Department of Physics and Astronomy and [†]Department of Chemistry and Biochemistry, Arizona State University, Tempe, Arizona 85287; [‡]Division of Basic Sciences, Arizona College of Osteopathic Medicine, Midwestern University, Glendale, Arizona 85308; [§]Laboratory of Receptor Biology and Gene Expression, National Cancer Institute, National Institutes of Health, Bethesda, Maryland 20892; and [¶]Biodesign Institute, Arizona State University, Tempe, Arizona 85287

ABSTRACT   In eukaryotes, genomic processes like transcription, replication, repair, and recombination typically require alterations in nucleosome structure on specific DNA regions to operate. ATP-dependent nucleosome remodeling complexes provide a major mechanism for carrying out such alterations in vivo. To learn more about the action of these important complexes, we have utilized an atomic force microscopy in situ technique that permits comparison of the same individual molecules before and after activation of a particular process, in this case nucleosome remodeling. This direct approach was used to look for changes induced by the action of the human Swi-Snf remodeling complex on individual, single-copy mouse mammary tumor virus promoter nucleosomal arrays. Using this technique, we detect a variety of changes on remodeling. Many of these changes are larger in scale than suggested from previous studies and involve a number of DNA-mediated events, including a preference for the removal of a complete turn (80 basepairs) of nucleosomal DNA. The latter result raises the possibility of an unanticipated mode of human Swi-Snf interaction with the nucleosome, namely via the 11-nm histone surface.

INTRODUCTION

Processes like transcription and replication require that specific factors access their appropriate DNA recognition sequences. The presence of nucleosomes typically restricts factor binding to DNA, resulting in an inhibition of these processes. Extensive study over the past decade has identified the actions of ATP-dependent nucleosome remodeling complexes such as Swi-Snf and effects mediated by covalent histone modifications like acetylation as the two major mechanisms whereby such nucleosome-mediated repression is relieved in vivo (Wolffe and Hayes, 1999; Flaus and Owen-Hughes, 2001; Becker and Horz, 2002; Berger, 2002; Narlikar et al., 2002; Tsukiyama, 2002; Fischle et al., 2003; Martens and Winston, 2003).

Several different types of ATP-dependent nucleosome remodeling complexes have been identified (Becker and Horz, 2002; Tsukiyama, 2002). Of these, the Swi-Snf family of complexes has probably been the most extensively studied (Becker and Horz, 2002; Narlikar et al., 2002; Martens and Winston, 2003). They have been shown to cause alterations in vitro that include enhanced accessibility of nucleosomal DNA to nuclease cleavage, histone octamer movement in *cis* (nucleosome sliding) or in *trans* (transfer between DNA molecules), formation of specific dinucleosome structures, and decreased levels of nucleosome-restrained supercoiling. Precisely how remodeling complexes carry out these alterations remains uncertain, but current models have converged on a mechanism in which the action of the remodeling complex triggers the release of a localized bulge of DNA that is propagated around the nucleosome, perhaps by DNA twisting or translocation activities inherent in the complex (Flaus and Owen-Hughes, 2001; Becker and Horz, 2002; Narlikar et al., 2002; Martens and Winston, 2003). This mechanism is proposed to account for most of the effects produced by these enzymes.

Single molecule approaches offer tremendous advantages for the study of complex and (apparently) heterogeneous processes such as nucleosome remodeling. However, to date, remodeling studies have been dominated by ensemble-average biochemical approaches, except for two single molecule analyses (Bazett-Jones et al., 1999; Schnitzler et al., 2001). In both cases, remodeling reactions were carried out in solution, and then the remodeled molecules were deposited for imaging. Thus, different molecules were analyzed before and after remodeling, and remodeling changes were assessed by comparing the two populations. In the work described here, we apply a single molecule atomic force microscopy (AFM) technique, first demonstrated by Kasas et al. (1997), which can detect events on individual molecules by imaging the same molecules before and after a process is activated. To apply this approach to nucleosome remodeling, chromatin arrays that had been preincubated with the remodeling complex human Swi-Snf (hSwi-Snf) under inactivating (no ATP) conditions are deposited and imaged in a flow cell linked to the AFM. After activation of hSwi-Snf by the addition of ATP, the same fields are reimaged. In this way, it is possible to study remodeling on individual chromatin molecules. Imaging is done in solution, which enhances the biological relevance of the results, and the system is physiologically relevant because single-copy

mouse mammary tumor virus (MMTV) promoter nucleosomal arrays reconstituted with human histones (Bash et al., 2003) are remodeled by the same complex that remodels this promoter in vivo during nuclear receptor mediated transcription activation (Yoshinaga et al., 1992; Muchardt and Yaniv, 1993; Fryer and Archer, 1998).

In an approach such as this one, the process takes place while the molecules are on the imaging surface, an environment that can inhibit enzyme activity (Kasas et al., 1997). However, for remodeling reactions carried out by hSwi-Snf, we find that many of the observed chromatin changes are more dramatic in scale than those previously suggested from biochemical or from single molecule studies. The changes are, however, consistent in nature with the types of remodeling outcomes suggested from those studies. The changes observed involve several novel DNA-mediated alterations in chromatin structure, including one that suggests an unanticipated mode of hSwi-Snf action.

MATERIALS AND METHODS

Chromatin analysis/hSwi-Snf remodeling

The hSWI/SNF complex was purified from the clone FL-INI1-11 (Sif et al., 1998) from cells grown by the National Cell Culture Center (NCCC, Minneapolis, MN). Nuclear extracts were prepared by the method of Dignam et al. (1983) and incubated with anti-Flag M2 affinity gels (Kodak, Rochester, NY) at 20 mg protein per 0.3 ml of affinity gel and washed extensively as described (Sif et al., 1998). Flag immobilized hSWI/SNF was then eluted with a 10-fold molar excess of Flag peptide in 20 mM HEPES (pH 7.9), 20% glycerol, 2 mM EDTA, 1 mM dithiothreitol (DTT), and 100 mM KCl for 1 h, and then stored at $-80°C$. The hSwi-Snf samples used contain bovine serum albumin (BSA) in a 4:1 molar ratio with hSwi-Snf (further reduction in BSA concentration greatly diminishes remodeling activity).

Nucleosomal arrays containing the MMTV promoter region were salt reconstituted to various subsaturated levels of nucleosome occupation with HeLa histones exactly as previously described (Bash et al., 2003) and then glutaraldehyde (GD) fixed, to prevent the loss of nucleosomes that occurs during solution imaging (Wang et al., 2002). Arrays were preincubated with hSwi-Snf, to avoid potential difficulties arising from diffusion-limited binding rates at these low sample concentrations, at stoichiometries ranging from 2.5 to 12 chromatin molecules per hSwi-Snf molecule for 20 min in a solution of 5 mM NaCl, 5 mM NaH_2PO_4 buffer (pH 7.5), and then deposited on GD-aminopropyltriethoxysilane (APTES); (Facci et al., 2002), derivatized at $1-\mu M$ levels with GD (substantially lower than in previous studies; Wang et al., 2002) and allowed to adsorb for a period of 40 min. After deposition, fields are scanned twice. The second scan assesses the effect of the AFM scanning process on chromatin structure and thus provides the background level of change. Thus, this important control is carried out on the same samples that will be analyzed for remodeling. Then a solution of 1 mM $MgCl_2$ and 1 mM ATP is flowed into the cell, and remodeling is allowed to take place for 30 min. Then the same fields (and the same set of tethered molecules) are scanned again, to determine the changes induced by hSwi-Snf remodeling. Other reaction times were tried, but 30 min was judged to be optimal. Note that since the Mg^{2+} and ATP are equimolar, there will be little free Mg^{2+} present (to affect chromatin structure). For imaging, the prepared sample is mounted into a scanning probe microscopy (SPM) liquid flow cell (Molecular Imaging, Phoenix, AZ.). Imaging was carried out with a Macmode PicoSPM (Molecular Imaging) equipped with Silicon Cantilevers (Maclevers type II, Molecular

Imaging) with a spring constant of 2.8 N/m. Measurements were performed at ~25 kHz driving frequency. The scanning rate was 1.78 Hz.

Data analysis

Pairs of images taken before and after ATP addition were compared by digital subtraction after alignment to compensate for instrumental drift. The difference images flagged changes that were then quantified using Scanning Probe Image Processor software (SPIP v3.0, Image Metrology, www.imagmet.com). Background levels of change were determined by comparing pairs of images taken in samples before ATP addition. Image pairs (pre- and post-ATP addition) were adjusted to approximately the same contrast scale, so that changes in the apparent width and height of features on ATP addition are real. These local changes are not analyzed here for two reasons. a), They may be produced by a trivial process such as changes in the AFM tip caused by picking up material freed during remodeling. b), Many of the distinctive local changes in the size of protein-like features may well reflect compositional changes on remodeling, but they cannot be identified without a means for identifying the proteins during imaging, a problem we are currently addressing.

The samples clearly lose rigidity during remodeling, and continuous scanning induces a higher level of scan-induced artifacts than this before and after imaging. Thus we cannot continuously track the remodeling process.

RESULTS

Flow-cell imaging of nucleosome remodeling

To study remodeling of individual chromatin molecules, nucleosomal arrays preincubated with human Swi-Snf are deposited on GD-APTES mica and imaged (twice to assess technique-induced changes; see Materials and Methods) in a flow-cell linked to the atomic force microscope. The GD-APTES surface tethers nucleosomes, probably via the lysines on the histone N-terminal tails, but leaves nucleosomal DNA free to move (Wang et al., 2002). To activate hSwi-Snf in the deposited chromatin sample, ATP is flowed into the cell and, after 30 min, the sample is reimaged. This combination of surface tethering and flow-cell imaging permits the very same nucleosomal arrays to be imaged before and after hSwi-Snf activation by ATP, thus allowing detection of remodeling events that have taken place on individual molecules.

Inspection of the images in Fig. 1 demonstrates that the method can reliably compare the same nucleosomal arrays before (Fig. 1 *a*) and after (Fig. 1 *b*) ATP is introduced into the flow cell. Indeed, the majority of molecules in the two images look exactly the same before and after ATP introduction. This lack of change could reflect the absence of remodeling or changes that are too subtle to be detectable by AFM; note that modest changes have been suggested from many previous remodeling studies (Becker and Horz, 2002; Narlikar et al., 2002). However, the +ATP images do contain array molecules that have clearly undergone significant alteration (compare the numbered molecules in the −ATP and +ATP scans; Fig. 1, *a* and *b*, respectively). Eight changes are marked on the full scans, and five examples of these are shown magnified to the right of the full
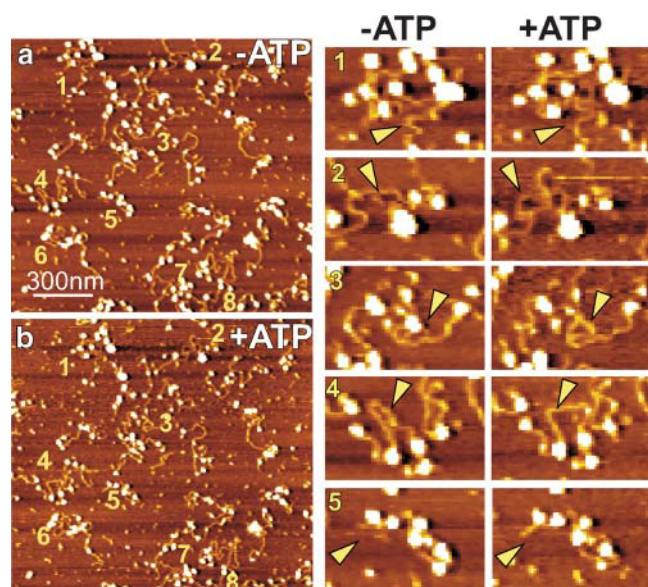
FIGURE 1   Analysis of hSwi-Snf action on MMTV chromatin arrays in situ. The two images in *a* and *b* show ~50% of one of the 70 or so fields (15–25 molecules per field) examined in this study. The top image (*a*) shows deposited chromatin/hSwi-Snf minus ATP, whereas the image below (*b*) shows the same field after ATP addition (the height scale is 11 nm). Numbers (*1–8*) are located next to molecules that demonstrate the types of major changes analyzed in this work. Five of these (numbered to correspond to the clusters in *a* and *b*) are shown at higher magnification in the pairs (−ATP, *left*; +ATP, *right*) of panels on the right of the figure. The yellow arrowheads in the panels point to changed regions. The histones and DNA are AFM pure (Wang et al., 2002; Bash et al., 2003), but the hSwi-Snf preparation contains BSA, which is required for hSwi-Snf activity. The particles that are smaller than normal nucleosome size could thus be BSA, dissociated histones, or hSwi-Snf subunits (see text). The particles that appear to be larger than nucleosomes, for example in Fig. 1 *b* (*1*), are roughly the size expected for intact hSwi-Snf (2×10^6 Da). We often note such particles near sites where major remodeling changes occur, but they cannot be unambiguously identified as hSwi-Snf based on their size alone. The hSwi-Snf/chromatin ratio is 1:6 for this pair of images.

scans. These images demonstrate that after ATP introduction array molecules show alterations in the free DNA path (1, 2, and 4–8), in the length of free DNA in particular regions (1–3 and 6–8), and in protein (nucleosome) size and position (2, 3, and 6–8). The changes we observe will be discussed in more detail below.

The additions of Mg^{2+} alone, ATP alone, or Mg^{2+} plus a nonhydrolyzable ATP derivative to identical tethered chromatin samples lacking hSwi-Snf produces no effects (not shown), i.e., the changes depend on hSwi-Snf activation by ATP.

These major changes are found in a minority of molecules, at least under the conditions used here (modest hSwi-Snf/chromatin ratios and tethered molecules). However, they are not rare, occurring in up to 10% of the molecules in a field. The frequency with which we observe them increases with increasing hSwi-Snf/chromatin ratios (*solid circles*, Fig. 2). On the other hand, chromatin changes resulting from the
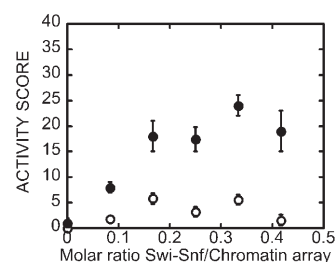

FIGURE 2   Dose response of MMTV promoter chromatin to hSwi-Snf. The ● plot remodeling activity (from the +ATP images) versus the molar ratio of Swi-Snf/chromatin molecules determined from the types of fields shown in Fig. 1. An activity score is defined as the number of individual nucleosomes that have undergone change (+ATP compared to −ATP) divided by the total number of chromatin molecules present in the image field. The hSwi-Snf/chromatin ratios range from 1:12.5 (0.08) to 1:2.5 (0.4). Error bars are ±1 SD. The ○ plot the background activity score as a function of hSwi-Snf/chromatin ratio. The background level of change is obtained by scanning the deposited hSwi-Snf/chromatin samples twice before ATP addition; the second scan assesses the level of changes in chromatin structure caused by the scanning process itself.

technique itself (tip induced movement in the sample during scanning, etc.) show no hSwi-Snf dose dependence (*open circles*, Fig. 2).

Classifying the major changes

Fig. 1 gives an indication of the variety of major changes that can be found in the +ATP images. The changes that individual molecules undergo are complex, and analyzing their precise nature is often difficult. This is true in large part because AFM, like most microscopy techniques, lacks the specificity to distinguish among different types of molecules. Thus, in heterogeneous systems like this one, which contain hSwi-Snf, nucleosomes, and BSA (in the hSwi-Snf preparation to maintain its activity), the various types of molecules appear the same; only their size could distinguish them. However, due to the possibility of hSwi-Snf and nucleosome dissociation, there could be size heterogeneity. Moreover, size in AFM techniques is tip dependent and therefore variable. Thus, size is not a reliable index to distinguish different types of molecules. Given this reality, we have focused on identifying the major changes that have occurred in the individual arrays −ATP versus +ATP. To do this, the images (−ATP/+ATP) were compared by digital subtraction and the flagged changes in the difference images analyzed using SPIP software. Using this analysis technique, we were able to group the major remodeling changes into four general classes: DNA or protein movement (*DM* or *PM*, Fig. 3 *a*), chromatin rewiring (*R*, Fig. 3, *b* and *c*), and DNA unwrapping from the nucleosome (*DU*, Fig. 3, *c* and *d*). Tracings to the right of each image pair illustrate these various types of changes. Grouping the changes into these four classes was useful for analysis purposes; we do not
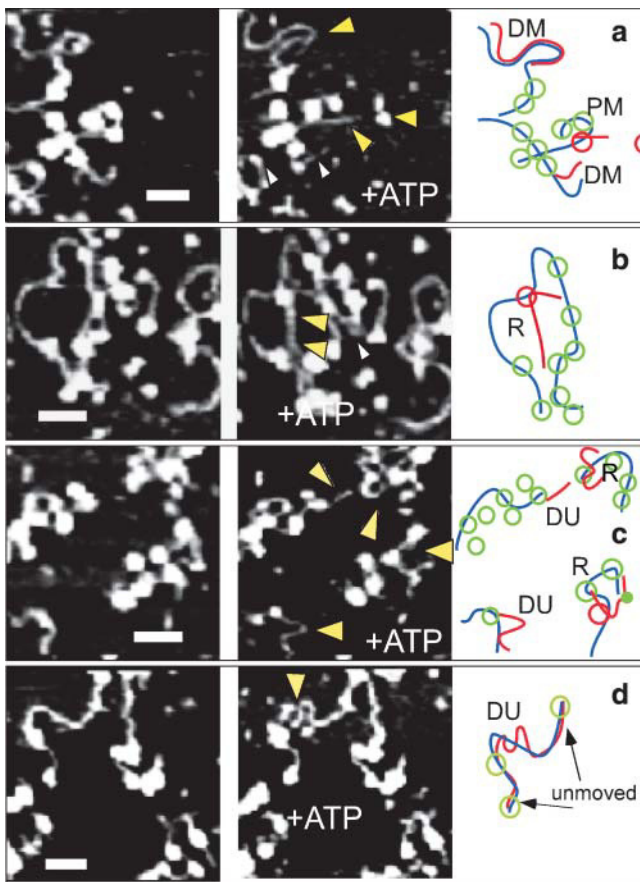
FIGURE 3 Specific examples of major remodeling changes. Panels *a*–*d* show various pairs of higher magnification images (enlarged from fields like the one shown in Fig. 1) that demonstrate the types of major changes detected in this work. The scale bars are 50 nm, and image widths vary from 175 to 220 nm. In all cases, the leftmost image is chromatin plus hSwi-Snf, deposited and imaged minus ATP, and the image to its right is the same field after ATP has been flowed into the cell (activating hSwi-Snf remodeling). Yellow arrowheads in the +ATP images mark the sites of major changes; there are also minor changes, some of which are marked with white arrowheads. Tracings to the right of each pair of images illustrate the major changes observed after ATP addition, by showing the path of the DNA (*blue*) and the locations of nucleosome-sized particles (*green* ○) or smaller particles (*green* ●) before ATP addition and the changes in DNA or protein caused by remodeling (*red*). Only major changes are marked in red. (*a*) DM/PM are events in which the DNA or protein shows a change in position relative to other molecules after ATP addition. Note that in Fig 3 *a*, there is both disappearance of protein and appearance of protein, indicated by red circles. (*b* and *c*) Rewiring events are characterized by new nucleosomal arrangements due to the transfer of DNA from one nucleosome to another, either within the same array molecule (in *cis,* panel *c*) or in a different array (in *trans*, panel *b*) and sometimes protein transfer (panel *b*). (*c* and *d*) DU events mark the appearance of new DNA (usually in or near a formerly nucleosomal region) and thus should reflect DNA unwrapping from the nucleosome. The particles much smaller than nucleosomes (cf. Fig. 3 *a*) are either hSwi-Snf subunits, dissociated histones such as H2A/H2B, or BSA. The hSwi-Snf/chromatin ratio is 1:6 (~1:25 hSwi-Snf/nucleosomes) for these images.

claim it provides a complete or detailed description of the complex events that occur upon remodeling.

In DM or PM events, DNA and/or protein has changed position in the +ATP image relative to the −ATP image, but the basic nucleosomal arrangements remain much the same; protein disappearance is also classed as a PM event (Fig. 3 *a*). For example, in Fig. 3 *a*, a cluster of trinucleosomes in the center and a stretch of DNA located near the top of the −ATP image are significantly altered in the +ATP image. The changes involve movements of DNA and protein, some disappearance of protein, and the appearance of a new length of DNA (*yellow arrowheads* in the +ATP image, and illustrated in a color-coded tracing to the *right* of the image pair). As is often the case, the presence of unaltered molecules (or individual nucleosomes) in the image provides useful referents that help insure correct identification of extensively remodeled molecules. R events reflect chromatin rearrangements that involve the transfer of DNA (and sometimes protein as well), either within the same (*cis*, Fig. 3 *c*) or to different (*trans*, Fig. 3 *b*) array molecules after ATP introduction. For example in Fig. 3 *b*, DNA and a nucleosome-sized protein structure appear de novo on a preexisting array (*yellow arrowheads*). In *cis* R events (Fig. 3 *c*, two cases), the DNA path within an array is altered. The ratio of *cis/trans* events in our data set is 24:7. Obviously, it is not possible to know if the rewired DNA in these R events is actually wrapped around the histone core as opposed to being merely associated with it. For example, branched structures (Fig. 3 *b*) seem unlikely to involve significant wrapping. In DU events, DNA appears in a localized region of the array after remodeling (typically very near the location of a nucleosome in the −ATP image), as judged by measuring DNA lengths in the region before and after ATP addition. In these events, the path of the DNA in the rest of the molecule usually remains unchanged (Fig. 3 *d*). DU events can occur either at the ends (*upper left arrowhead*) or internal regions (*lower left arrowhead*, Fig. 3 *c*) of an array. As mentioned above, for any of these four types of changes, it is not always possible to make a complete characterization, e.g., where DNA comes from in R events like Fig. 3 *b*, but the ability to analyze the same molecules before and after ATP introduction makes it unambiguously apparent that significant alterations have occurred on that molecule. The R events are difficult to characterize because of their dramatic nature. It is important to mention that R and DU classes of events can only result from ATP-dependent hSwi-Snf remodeling (see below). Additional R and DU events are shown in Supplemental Fig. 1. We detected little evidence for nucleosome sliding, a commonly suggested remodeling outcome. This could be due to the tethering of nucleosomes to the surface in our experiments.

This variety of major chromatin changes that are observed after hSwi-Snf activation not only takes place within a single chromatin sample but even occurs in individual molecules that are in close spatial proximity (cf. Fig. 3, *a* and *c*, and

Supplemental Fig. 1, *c* and *d*), thus demonstrating that hSwi-Snf is inherently capable of producing different types of remodeling outcomes.

Modest remodeling events (Fig. 3 *a*, *white arrowhead*) also occur in molecules that lie close to molecules undergoing major changes, indicating that variability in remodeling extent is also a characteristic of hSwi-Snf action. Such heterogeneity makes single molecule techniques particularly appropriate for studying the process of nucleosome remodeling. We did not analyze the more modest remodeling changes because some of them could result from scanning-induced changes (see Materials and Methods) and because the large-scale changes are the most novel.

The arrays shown in Figs. 1 and 3 contain an average of 4.4 nucleosomes per template. More highly loaded MMTV arrays (averaging 7.6 nucleosomes per template) undergo remodeling changes that are quite similar to those shown above (data not shown), but the changes are more difficult to analyze due to the higher nucleosome density on the arrays. In addition, these samples show an increased incidence of large and highly compacted structures (Fig. 4). These structures result from the presence of hSwi-Snf (they are not observed without hSwi-Snf and are present in both plus and minus ATP); similar structures were detected in the ex situ AFM studies of Schniztler et al. (2001). The structures show evidence of remodeling changes (Fig. 4) but they are impossible to analyze by AFM. For the above reasons, the less highly loaded array samples ($n_{av} = 4.4$) were used for the detailed quantitative analyses presented below. The similarity in the types of remodeling changes observed in both the highly loaded arrays (in the uncompacted molecules) and less highly loaded arrays argues that the changes we observe are characteristic of chromatin at any occupation level.

Quantifying the major remodeling changes

The overall frequency of major changes (all four classes) observed after hSwi-Snf activation is typically >10-fold higher than the level of background change (Fig. 2). The frequency of changes suggests that hSwi-Snf is acting catalytically in our system. For example, samples with a hSwi-Snf/chromatin ratio of 1:6 (0.17) contain an ~25-fold molar excess of nucleosomes over hSwi-Snf molecules on a per nucleosome basis, yet 5–10% of the nucleosomes in a given field undergo major changes, in addition to many (unscored) minor changes. These changes do not reverse when ATP is removed (data not shown), which is also consistent with catalytic action of hSwi-Snf (Imbalzano et al., 1996).

The relative frequencies of each of the four classes of major remodeling changes are shown in Fig. 5 *a*. DNA unwrapping (*DU*) and chromatin rewiring (*R*) are the two most common changes observed (*dotted bars*) but these two are not observed at all in the background (−ATP) scans (*solid gray bars*). Thus, they must result from ATP-dependent hSwi-Snf remodeling. In addition, PM and especially DM changes occur more frequently after hSwi-Snf activation. The R and DU frequencies shown are a minimal estimate because they were only scored as R and DU events if changes were unambiguous. For example, some PM events could in fact be R events, and many changes were unscored because the exact nature of the change was ambiguous.

Rewiring is both the most frequent and most dramatic class of events, as well as the most difficult to characterize. On the other hand, DNA unwrapping changes are clear enough to be analyzed quantitatively. This analysis makes a very interesting point; the most commonly observed DNA
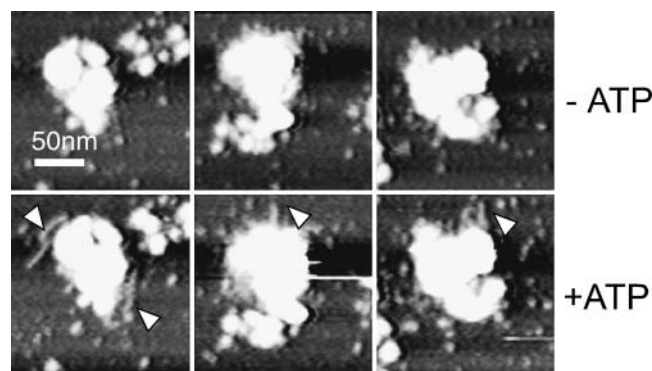

FIGURE 4 Remodeling changes in more highly occupied nucleosomal arrays. This figure shows examples of the types of compacted structures observed in images of more highly occupied MMTV arrays in the presence of hSwi-Snf. Comparison of the −ATP and +ATP samples shows clear evidence of remodeling, as free DNA is released from the globs (arrowheads). Without hSwi-Snf, there are no compacted structures in this sample (not shown).
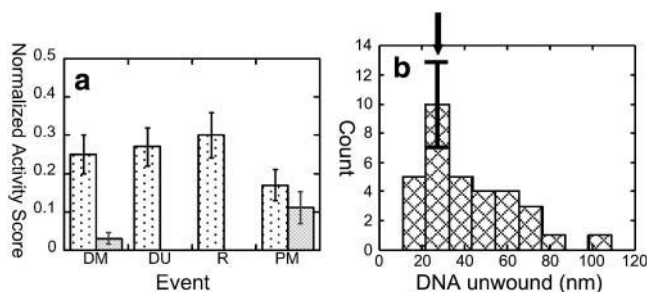

FIGURE 5 Quantifying hSwi-Snf remodeling events. The dotted bars in *a* show the normalized (total = 1) frequencies of changes produced by remodeling, i.e., after ATP addition, for each of the categories of change exemplified in Fig. 3: DNA movement (*DM*), protein movement (*PM*), DNA unwrapping (*DU*), and chromatin rewiring (*R*). The solid gray bars show the background levels for each category of change, obtained from repetitive scans (see Materials and Methods) of chromatin samples plus hSwi-Snf but minus ATP. These are normalized values, relative to the +ATP (remodeled) values. Error bars are ±1 SD. Panel *b* shows a histogram of the lengths of DNA unwrapped from nucleosomes (DU events) after ATP addition. The most populated bin corresponds to 22–33 nm (~65–97 bp). The arrow marks the length of DNA that corresponds to one turn around the nucleosome core (80 bp). The error bar indicates ±1 SD on the peak count.

lengths observed in DU events are ~65–97 basepairs (bp) (Fig. 5 b, 20–30 nm bin). This length corresponds roughly to one turn of nucleosomal DNA (80 bp). Thus, hSwi-Snf apparently has a preference for unwrapping a complete turn of nucleosomal DNA during remodeling. That the DNA (loops) were directly removed from the nucleosome itself rather than additional DNA being pulled or otherwise propagated through flanking nucleosomes is indicated by the observation that the paths of DNA on each side of the event (i.e., the DNA stretches that are adjacent to the released segment) typically show no change (e.g., Fig. 3, c and d); it seems unlikely that DNA could be pulled through neighboring tethered nucleosomes without changing the DNA path somewhere within the array. The release of such fairly significant amounts of DNA from nucleosomes by hSwi-Snf is consistent with other observations: remodeling changes across large regions of the nucleosome (Aoyagi et al., 2002); significant local (Gavin et al., 2001) topological changes during remodeling on circular arrays (Gavin et al., 2001; Guyon et al., 2001), and the release of a ''writhe of protein-free DNA'' from a nucleosome, detected by electron microscopy (Fig. 4 b of Bazett-Jones et al., 1999).

DISCUSSION

We have utilized an AFM approach that can analyze complex biological processes at the level of individual molecules to study the action of the ATP-dependent nucleosome remodeling complex hSwi-Snf on subsaturated MMTV promoter chromatin arrays. The remodeling changes that we visualize are consistent with the types of changes observed in previous in vitro studies of Swi-Snf remodeling (Flaus and Owen-Hughes, 2001; Becker and Horz, 2002; Narlikar et al., 2002; Martens and Winston, 2003): enhanced accessibility of nucleosomal DNA to nuclease cleavage, decreased restrained supercoiling (as loops of DNA are released from nucleosomes), and nucleosome movements in cis and in trans. The novelty of our results lie 1), in the magnitudes of many of the individual remodeling changes, which are significantly larger than typically suggested from previous studies and 2), in the nature and variety of DNA-mediated remodeling changes. We also see evidence consistent with the more modest types of remodeling events proposed previously. There may be several possible reasons why such significant changes have not previously been reported:

i. Experimental approach. The technique we use can analyze the same molecules before and after hSwi-Snf activation. This approach provides direct information about remodeling changes on individual nucleosomal arrays. Such comparisons were not possible in previous remodeling studies, even the single molecule ones, and unambiguous identification of these major changes as specific remodeling events would have been impossible

without this capability. Moreover, ensemble-average approaches (used in biochemical studies) could miss major changes that occur in a fraction of the population or score them differently. For example, the types of large-scale DNA changes (DM, R, and DU) that we observe should significantly enhance restriction enzyme accessibilities (a common diagnostic for remodeling) in a subset of nucleosomal arrays although a majority of the arrays maintain their octamers, due to modest or no remodeling. Heterogeneity in remodeling outcomes makes single molecule techniques that can track events on individual molecules particularly appropriate for analyzing remodeling, and this seems to us to be the most likely reason we detect these large-scale events.

ii. Template differences. The chromatin fragments we use are reconstituted on a DNA template that has physiological significance because this DNA is a normal target of hSwi-Snf remodeling in vivo (Fryer and Archer, 1998). Moreover, its physical properties do differ significantly (Bash et al., 2003) from those of the concatameric 5S templates typically used for in vitro remodeling studies. Our studies also use subsaturated arrays, which is necessary both for the AFM approach and to be able to use this physiologically relevant template (Bash et al., 2003). However, the remodeling changes that we observe do not appear to depend on array occupation level since we observe similar remodeling events on arrays at various occupation levels.

iii. Surface effects. Surface tethering of chromatin and the possible binding of hSwi-Snf to the surface may impact our studies. For example, histone tethering seems likely to suppress changes that involve histone movement or transfer (though histone loss from tethered arrays has been observed; Bash et al., 2003), so there may be classes of remodeling activities that are missed in our experiments. Also, chromatin fixation, which is necessary to avoid histone loss and has been used in previous studies (Schnitzler et al., 2001), could affect the results. However, all these constraints would be expected to temper the action of hSwi-Snf, not to enhance it, relative to remodeling in solution. Therefore, the observation of larger scale changes is counter to the expected artifactual influences of the above constraints. Because our system is likely to mitigate the action of remodeling complexes, one might anticipate that hSwi-Snf would be capable of this degree or perhaps even a larger scale of remodeling action in vivo.

The analysis detects a significant incidence of DNA-mediated remodeling changes: DNA transfer in cis or trans, DNA unwrapping from nucleosomes, and DNA movement. Although the tendency of hSwi-Snf to carry out these types of reactions may be exaggerated by surface tethering of the histones, the observations do demonstrate that remodeling
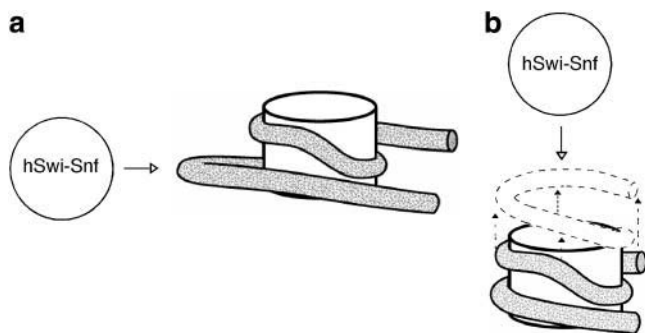
complexes like hSwi-Snf are capable of carrying out major alterations directly through DNA. This is consistent with their proven ability to break histone-DNA contacts although not affecting histone octamer structure (Bazett-Jones et al., 1999). An ability to carry out alterations directly via nucleosomal DNA would provide an easy, direct, and potentially quite reversible way for Swi-Snf complexes to alter chromatin organization to facilitate DNA access and could prove useful in various types of in vivo genomic processes.

The observed preference of hSwi-Snf to remove a complete turn of nucleosomal DNA is particularly intriguing. Current models (Flaus and Owen-Hughes, 2001; Becker and Horz, 2002; Narlikar et al., 2002; Martens and Winston, 2003) propose that remodeling complexes work by propagating a bulge of released DNA around the nucleosome, acting via its 5-nm DNA-containing face (Fig. 6 a) and possibly initiating their action at the nucleosomal DNA entry/exit sites. However, this mechanism seems unlikely to produce a preference for releasing complete 80-bp turns of DNA. On the other hand, hSwi-Snf acting through the 11-nm histone surface of the nucleosomal disc (Fig. 6 b), perhaps lifting off a turn of DNA, could produce such a preference. The likely tendency of nucleosomes to lie flat on the imaging surface would preferentially expose the 11-nm face and thus might enhance this mode of approach in our studies; however, this approach mechanism is also consistent with solution observations. For example, H3-H4 tetramer-DNA complexes are not as efficiently remodeled as complete nucleosomes (Boyer et al., 2000). Tetramer complexes lack H2A and H2B, which are significant features of the 11-nm face of the complete nucleosome (Luger et al., 1997) and thus ought to be viewed differently by remodeling complexes that approach via this surface. An electron microscopy imaging model of yeast Swi-Snf shows the complex to be oblate in shape with a cavity capable of accommodating the 11-nm nucleosome face (Smith et al., 2003). This approach mechanism is consistent with the ability of Swi-Snf to remodel nucleosomal DNA containing nicks (Aoyagi and Hayes, 2002) that should compromise DNA torsion-dependent remodeling mechanisms. Nucleosomes can contact each other via the 11-nm surface (Luger et al., 1997). Other factors that interact with nucleosomes might also use this mode of contact; for example, H2A-H2B dimers would be readily accessible on the 11-nm surface for mobilization by FACT, a complex that facilitates chromatin transcription (Belotserkovskaya et al., 2003).

In summary, we have used a technique that can study biological processes in individual molecules to analyze nucleosome remodeling by the ATP-dependent nucleosome remodeling complex hSwi-Snf. We find that this complex has an intrinsic ability to carry out a variety of major remodeling changes, some of which are previously unreported. Such variety might be a useful property considering the many in vivo processes in which these remodelers appear to function. If remodeling complexes can carry out major remodeling activities in vivo that are similar to those we observe here, they will have the potential to be able to make significant alterations in in vivo chromatin structure. Our results also provide evidence for a mechanism of hSwi-Snf action that differs from those previously suggested for remodeling complexes, which may indicate that these complexes can use a variety of mechanisms to carry out remodeling. The heterogeneities inherent in hSwi-Snf action make single molecule approaches like the one used here particularly appropriate for studying their activities. Our conclusions are subject to the usual caveats of a surface microscopy approach. Nonetheless, the results are novel, striking, and their validity subject to testing by other (cf. biochemical) methods. This type of approach could prove useful for studying other complex biological processes at single molecule resolution.

SUPPLEMENTARY MATERIAL

An online supplement to this article can be found by visiting BJ Online at http://www.biophysj.org.

FIGURE 6 Possible mechanisms of hSwi-Snf action. Two options for hSwi-Snf approach and interaction with the nucleosome are illustrated. In a, a bulge of dissociated DNA is created by hSwi-Snf acting through the 5-nm, DNA containing face of the nucleosome. Panel b illustrates hSwi-Snf acting through the 11-nm histone surface of the nucleosome and releasing an ~80-bp turn of nucleosomal DNA, shown as a dashed circle. The method of representing the nucleosome was adapted from Fig. 3 in Narlikar et al. (2002).

REFERENCES

Aoyagi, S., and J. J. Hayes, 2002. hSWI/SNF-catalyzed nucleosome sliding does not occur solely via a twist-diffusion mechanism. Mol. Cell. Biol. 22:7484–7490.

Aoyagi, S., G. Narlikar, C. Zheng, S. Sif, R. E. Kingston, and J. J. Hayes. 2002. Nucleosome remodeling by the human SWI/SNF complex requires transient global disruption of histone-DNA interactions. Mol. Cell. Biol. 22:3653–3662.

Bash, R., H. Wang, J. Yodh, G. Hager, S. M. Lindsay, and D. Lohr. 2003. Nucleosomal arrays can be salt-reconstituted on a single-copy MMTV

promoter DNA template: their properties differ in several ways from those of comparable 5S concatameric arrays. *Biochemistry*. 42:4681–4690.

Bazett-Jones, D. P., J. Cote, C. C. Landel, C. L. Peterson, and J. L. Workman. 1999. The SWI/SNF complex creates loop domains in DNA and polynucleosome arrays and can disrupt DNA-histone contacts within these domains. *Mol. Cell. Biol.* 19:1470–1478.

Becker, P. B., and W. Horz. 2002. ATP-dependent nucleosome remodeling. *Annu. Rev. Biochem.* 71:247–273.

Belotserkovskaya, R., S. Oh, V. A. Bondarenko, G. Orphanides, V. M. Studitsky, and D. Reinberg. 2003. FACT facilitates transcription-dependent nucleosome alteration. *Science*. 301:1090–1093.

Berger, S. 2002. Histone modifications in transcriptional regulation. *Curr. Opin. Gen. Dev.* 12:142–148.

Boyer, L. A., X. Shao, R. H. Ebright, and C. L. Peterson. 2000. Roles of the histone H2A-H2B dimers and the (H3-H4)(2) tetramer in nucleosome remodeling by the SWI-SNF complex. *J. Biol. Chem.* 275:11545–11552.

Dignam, J. D., R. M. Lebovitz, and R. G. Roeder. 1983. Accurate transcription initiation by RNA polymerase II in a soluble extract from isolated mammalian nuclei. *Nucleic Acids Res.* 11:1475–1489.

Facci, P., D. Alliata, L. Andolfi, B. Schnyder, and R. Kotz. 2002. Formation and characterization of protein monolayers on oxygen-exposing surfaces by multiple-step self-chemisorption. Surface Science. 504:282–292.

Fischle, W., Y. Wang, and C. D. Allis. 2003. Histone and chromatin cross-talk. *Curr. Opin. Cell Biol.* 15:172–183.

Flaus, A., and T. Owen-Hughes. 2001. Mechanisms for ATP-dependent chromatin remodelling. *Curr. Opin. Genet. Dev.* 11:148–154.

Fryer, C. J., and T. K. Archer. 1998. Chromatin remodelling by the glucocorticoid receptor requires the BRG1 complex. *Nature*. 393:88–91.

Gavin, I., P. J. Horn, and C. L. Peterson. 2001. SWI/SNF chromatin remodeling requires changes in DNA topology. *Mol. Cell.* 7:97–104.

Guyon, J. R., G. J. Narlikar, E. K. Sullivan, and R. E. Kingston. 2001. Stability of a human SWI-SNF remodeled nucleosomal array. *Mol. Cell. Biol.* 21:1132–1144.

Imbalzano, A. N., G. R. Schnitzler, and R. E. Kingston. 1996. Nucleosome disruption by human SWI/SNF is maintained in the absence of continued ATP hydrolysis. *J. Biol. Chem.* 271:20726–20733.

Kasas, S., N. H. Thomson, B. L. Smith, H. G. Hansma, X. Zhu, M. Guthold, C. Bustamante, E. T. Kool, M. Kashlev, and P. K. Hansma. 1997. Escherichia coli RNA polymerase activity observed using atomic force microscopy. *Biochemistry*. 36:461–468.

Luger, K., A. W. Mader, R. K. Richmond, D. F. Sargent, and T. J. Richmond. 1997. Crystal structure of the nucleosome core particle at 2.8 A resolution. *Nature*. 389:251–260.

Martens, J. A., and F. Winston. 2003. Recent advances in understanding chromatin remodeling by Swi/Snf complexes. *Curr. Opin. Gen. Dev.* 13:136–142.

Muchardt, C., and M. Yaniv. 1993. A human homologue of Saccharomyces cerevisiae SNF2/SWI2 and Drosophila brm genes potentiates transcriptional activation by the glucocorticoid receptor. *EMBO J.* 12:4279–4290.

Narlikar, G. J., H. Y. Fan, and R. E. Kingston. 2002. Cooperation between complexes that regulate chromatin structure and transcription. *Cell*. 108:475–487.

Schnitzler, G. R., C. L. Cheung, J. H. Hafner, A. J. Saurin, R. E. Kingston, and C. M. Lieber. 2001. Direct imaging of human SWI/SNF-remodeled mono- and polynucleosomes by atomic force microscopy employing carbon nanotube tips. *Mol. Cell. Biol.* 21:8504–8511.

Sif, S., P. T. Stukenberg, M. W. Kirschner, and R. E. Kingston. 1998. Mitotic inactivation of a human SWI/SNF chromatin remodeling complex. *Genes Dev.* 12:2842–2851.

Smith, C. L., R. Horowitz-Scherer, J. F. Flanagan, C. L. Woodcock, and C. L. Peterson. 2003. Structural analysis of the yeast SWI/SNF chromatin remodeling complex. *Nat. Struct. Biol.* 10:141–145.

Tsukiyama, T. 2002. The in vivo functions of ATP-dependent chromatin-remodelling factors. *Nat. Rev. Mol. Cell. Biol.* 3:422–429.

Wang, H., R. Bash, J. G. Yodh, G. L. Hager, D. Lohr, and S. M. Lindsay. 2002. Glutaraldehyde modified mica: a new surface for atomic force microscopy of chromatin. *Biophys. J.* 83:3619–3625.

Wolffe, A. P., and J. J. Hayes. 1999. Chromatin disruption and modification. *Nucleic Acids Res.* 27:711–720.

Yoshinaga, S. K., C. L. Peterson, I. Herskowitz, and K. R. Yamamoto. 1992. Roles of SWI1, SWI2, and SWI3 proteins for transcriptional enhancement by steroid receptors. *Science*. 258:1598–1604.